The Standard Model

Contents

The Standard Model

The Standard Model of particle physics provides the most accurate description of nature at the subatomic level. It is based on the quantum theory of fields and has been tested with exquisite precision. In the quantum field theory there is one field for each type of particle – matter particles and force particles.

1 Matter particles

The fundamental matter particles in the Standard Model are the **quarks** and the **leptons**. All are spin-half point-like fermions.

We introduced the six quarks in §**??** their distinguishing characteristic is that they are charged ('coloured') under the strong force and as a result they are always found to be confined within hadrons.

The second class of matter particles is the **leptons**. These are also spin-$\frac{1}{2}$ fermions but unlike the quarks they do not have any strong interactions, because they carry no colour charge. Like the quarks, there are three families of leptons. The lightest generation (or family) contains the electron e^- and its partner neutrino ν_e.

The second generation consists of the muon μ^- and its partner neutrino ν_μ. The muon is very similar to the electron with the same $(\mathcal{Q} = -1)$ electric charge, but is about 200 times heavier. The larger mass of the muon means that it accelerates less than the electron in electric fields, therefore it emits less electromagnetic radiation than the electron when passing through material. Muons are therefore highly penetrating. High energy muons created in the upper atmosphere are able to pass through the atmosphere and can be observed on the earth's surface. The muon lifetime is $2.2\,\mu s$ after which it decays as follows

$$\mu^- \rightarrow e^- + \bar{\nu}_e + \nu_\mu.$$

The third generation contains the tau τ^- and its neutrino ν_τ. The tau also has $\mathcal{Q} = -1$, and is heavier again: about 3,500 times heavier than the electron. The tau lepton decays very rapidly in 2.9×10^{-13} s. It can decay to either an electron or a muon (plus associated neutrinos)

$$\begin{aligned} \tau^- &\rightarrow e^- + \bar{\nu}_e + \nu_\tau \\ \tau^- &\rightarrow \mu^- + \bar{\nu}_\mu + \nu_\tau \end{aligned}$$

These are not the only options. Because the τ has a mass larger than many hadrons,

	Quarks		Leptons	
Generation	$\mathcal{Q} = -\frac{1}{3}$	$\mathcal{Q} = +\frac{2}{3}$	$\mathcal{Q} = -1$	$\mathcal{Q} = 0$
First	down (d) $\sim$ 5 MeV	up (u) $\sim$ 2.5 MeV	electron (e) 0.511 MeV	e neutrino (ν_e) < 1 eV
Second	strange (s) ~ 101 MeV	charm (c) 1270 MeV	muon (μ) 105.7 MeV	μ neutrino (ν_μ) < 1 eV
Third	bottom (b) 4200 MeV	top (t) 172 GeV	tau (τ) 1777 MeV	τ neutrino (ν_τ) < 1 eV

Table 1: The quark and lepton families, their masses and their charges $\mathcal{Q}$. All are spin-$\frac{1}{2}$ fermions. The corresponding anti-particles have the same masses as the particles, but the opposite charges. The fermionic particles have positive parity while their anti-particles have negative parity.

it also decays into hadrons, through reactions such as

$$\begin{aligned}
\tau^- &\to \pi^- + \nu_\tau \\
\tau^- &\to \pi^- + \pi^0 + \nu_\tau \\
\tau^- &\to \pi^- + \pi^+ + \pi^- + \nu_\tau \\
\tau^- &\to K^- + \nu_\tau .
\end{aligned}$$

A summary of the some of the most important properties of the six quarks and six leptons can be found in Table 1.

1.1 Lepton flavour number

It is useful to define quantum numbers that count the number of leptons. Associated with each lepton is an anti-lepton. We can define **lepton flavour numbers** to be the number of leptons of each generation less the number of corresponding anti-leptons in that generation:

$$\begin{aligned}
L_e &= N(e^-) + N(\nu_e) - N(e^+) - N(\bar{\nu}_e) \\
L_\mu &= N(\mu^-) + N(\nu_\mu) - N(\mu^+) - N(\bar{\nu}_\mu) \\
L_\tau &= N(\tau^-) + N(\nu_\tau) - N(\tau^+) - N(\bar{\nu}_\tau)
\end{aligned}$$

We can also define a **total lepton number** $L_\ell = L_e + L_\mu + L_\tau$. Total lepton number is conserved in all known reactions. The individual lepton flavour numbers are also conserved in most reactions. The exception is in the phenomenon of neutrino oscillation, which we shall meet later (§5).

Force	Quantum	Symbol	Mass	Spin	α	Range
Electromagnetic	Photon	γ	0	1	$\frac{1}{137}$	∞
Strong	Gluon ($\times 8$)	g	0	1	~ 1	$\sim 10^{-15}$ m
Weak	$W^{\pm}$		80.4 GeV	1	$\frac{1}{29}$	$\sim 10^{-18}$ m
	Z^0		91.2 GeV	1		
Gravity	Graviton?	G	0	2?		∞

Table 2: The force-carrying particles γ, g, $W^{\pm}$ and Z^0 of the Standard Model. The spin is in units of $\hbar$. The symbol α indicates the corresponding dimensionless 'fine structure constant'.

2 Force particles

There are four fundamental forces which act on the matter particles (Table 2). They are: electromagnetism, the weak nuclear force, the strong nuclear force and gravity.

The gravitational force is a special case. It is very familiar, but at the level of individual subatomic particles is so much weaker than the other forces that it has a negligible effect. This makes it difficult to study, and so the microscopic mechanism behind gravitation is yet to be fully understood. We will not discuss it further in this course.

Each of the other three forces is known to be carried by an intermediate particle or particles. The mediating particles are excitations of the associated fields and are **spin-1 bosons**.

The quantum of the electromagnetic force is the **photon**, which is a massless boson with no electrical charge. It is through virtual photons that electromagnetic forces are transmitted between charges. The scattering process by virtual photons is described in §**??**. The quantum theory of electromagnetism is known as **quantum electrodymanics** or QED.

The electromagnetic interaction is felt by all charged particles. The vertex factor for a particle of with charge quantum number $\mathcal{Q}$ is $\mathcal{Q}g_{\rm EM}$ where $\frac{g_{\rm EM}^2}{4\pi} = \alpha_{\rm EM}$. For example, the u-quark has charge $\mathcal{Q} = \frac{2}{3}$, so the coupling strength in the $uu\gamma$ vertex

is only two thirds as large as that in the $ee\gamma$ vertex, and of the opposite sign.

The electromagnetic interaction does not change quark flavour, nor lepton flavour. Flavour-changing vertices such as:

$$\mu^- + \gamma \not\rightarrow e^- \qquad \text{[violates lepton flavour - forbidden}$$
$$u + \gamma \not\rightarrow c \qquad \text{[violates quark flavour - forbidden}$$

are forbidden in electromagnetism.

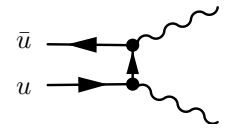

Feynman diagram for neutral pion decay

Decays which do not require changes in flavour quantum numbers may proceed via the electromagnetic interaction, for example the decay of the neutral pion to two photons

$$\pi^0 \longrightarrow \gamma + \gamma.$$

Another example is the decay of the Σ^0 baryon to the Λ^0 baryon, both of which having quark content uds,

$$\Sigma^0 \longrightarrow \Lambda^0 + \gamma.$$

3 The strong force and the gluon

The quantum theory of the strong force is known as **quantum chromodynamics** or QCD. The strong force is mediated by spin-1, massless particles known as **gluons**. The gluons couple to colour charge, rather like the photons couple to electromagnetic charge. Since the leptons have no colour charge, they do not interact with gluons, and hence do not interact via the strong force.

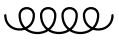
Gluon line.

Quarks carry colour, r, g and b. Anti-quarks carry anti-colour $\bar{r}$, $\bar{g}$ and $\bar{b}$. Each gluon carries both colour and anti-colour. We might then think that there should be $3 \times 3 = 9$ gluons. However one of those nine combinations

$$\frac{1}{\sqrt{3}}(|r\bar{r}\rangle + |g\bar{g}\rangle + |b\bar{b}\rangle)$$

is colourless, and so there are $3^2 - 1 = 8$ orthogonal gluon states. Total colour charge is conserved at each vertex, with any change in the colour of the quark being introduced or carried away by the gluon.

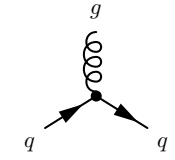

A quark-gluon vertex

The strong interaction has a larger coupling constant than the electromagnetic force

$$\alpha_S \sim 1 \qquad \text{whereas} \qquad \alpha_{\rm EM} \approx \frac{1}{137},$$

meaning that if both forces are present, the strong force tends to dominate. The largeness of the strong coupling constant g_S also means that if a reaction can occur both through the strong force and the electromagnetic force, the strong force reaction can be expected to dominate.

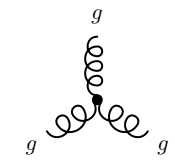

Three-gluon vertex

However the strong force is more than just a stronger version of the electromagnetic interaction. Gluons (unlike photons) can act as sources for their own field. This

A precise theory

Non-examinable

Quantum electrodynamics has been tested to amazing accuracy. The most precise measurement is of the gyromagnetic ratio g_e of the electron. We define g by the equation

$$\boldsymbol{\mu} = -\frac{g}{2}\frac{e}{m_e}\mathbf{s}$$

where $\boldsymbol{\mu}$ is the electron's magnetic moment, e is the magnitude of its charge, and $\mathbf{s}$ is its spin. The Dirac theory of electromagnetism predicts that

$$g_e^{\mathrm{dirac}} = 2.$$

The Dirac theory prediction is the value obtained by considering the direct coupling of photons to the charge. If one includes the one-loop correction, the prediction can be refined to

$$g_e^{\mathrm{one-loop}}/2 = 1 + \frac{1}{2}\frac{\alpha_{\mathrm{EM}}}{\pi} \approx 1.0011$$

The experimental and theoretical measurements have been improving in precision almost in parallel, competing for higher precision. The current best experimental measurement [Hanneke(2008)] has been made with the extraordinary accuracy of better than one part per trillion:

$$g^{\mathrm{experiment}}/2 = 1.001\,159\,652\,180\,7\,(3),$$

where the number in brackets shows the uncertainty in the last digit.
To achieve this level of accuracy in the theory, one must calculate a very large number of Feynman diagrams (there are 891 four-loop diagrams and 12672 five-loop diagrams). The five-loop theoretical calculation [Aoyama(2012)] was completed in 2012, giving

$$g^{\mathrm{theory}}/2 = 1.001\,159\,652\,181\,8\,(8),$$

in agreement with the experimental measurement.

Why eight gluons?

Non-examinable

There are three colours of quarks, which we have labelled r, g and b. We can place them in a basis such that:

$$|r\rangle = \begin{pmatrix} 1 \\ 0 \\ 0 \end{pmatrix} \qquad |g\rangle = \begin{pmatrix} 0 \\ 1 \\ 0 \end{pmatrix} \qquad |b\rangle = \begin{pmatrix} 0 \\ 0 \\ 1 \end{pmatrix}$$

Colour forms a 3-dimensional Hilbert space, and so for colour transformations, induced by gluons, we want the set of linear operators on that space. This can be represented by the group of 3×3 unitary matrices with unit determinant, which is called $SU(3)$.

A group $SU(N)$ has $N^2 - 1$ degrees of freedom (the -1 coming from the requirement of unit determinant). There are therefore $2^2 - 1 = 3$ Pauli matrices acting on the two-dimensional Hilbert space for a spin-half particle. There are $3^2 - 1 = 8$ generators of $SU(3)$ for the three-dimensional complex space of colour. The eight matrices $\{T_1, T_2, \ldots T_8\}$ are the generators and are traceless, Hermitian matrices. They can be represented by $T_a = i\frac{1}{2}\lambda_a$, where the λ_a are the Gell-Mann matrices

$$\lambda_1 = \begin{pmatrix} 0 & 1 & 0 \\ 1 & 0 & 0 \\ 0 & 0 & 0 \end{pmatrix} \qquad \lambda_2 = \begin{pmatrix} 0 & -i & 0 \\ +i & 0 & 0 \\ 0 & 0 & 0 \end{pmatrix} \qquad \lambda_3 = \begin{pmatrix} 1 & 0 & 0 \\ 0 & -1 & 0 \\ 0 & 0 & 0 \end{pmatrix}$$

$$\lambda_4 = \begin{pmatrix} 0 & 0 & 1 \\ 0 & 0 & 0 \\ 1 & 0 & 0 \end{pmatrix} \qquad \lambda_5 = \begin{pmatrix} 0 & 0 & -i \\ 0 & 0 & 0 \\ i & 0 & 0 \end{pmatrix} \qquad \lambda_6 = \begin{pmatrix} 0 & 0 & 0 \\ 0 & 0 & 1 \\ 0 & 1 & 0 \end{pmatrix}$$

$$\lambda_7 = \begin{pmatrix} 0 & 0 & 0 \\ 0 & 0 & -i \\ 0 & +i & 0 \end{pmatrix} \qquad \lambda_8 = \begin{pmatrix} 1 & 0 & 0 \\ 0 & 1 & 0 \\ 0 & 0 & -2 \end{pmatrix}$$

the three-dimensional analogues of the Pauli matrices. A transformation in colour space can then be represented by the unitary transformation

$$|\Psi\rangle \longrightarrow \exp\left(\vec{\lambda} \cdot \vec{\alpha}\right) |\Psi\rangle$$

for some eight-dimensional vector $\vec{\alpha}$.

means that there is a gluon self-interaction force, involving a three-gluon interaction vertex. This makes a dramatic difference to the way the strong force works.

The self-interactions of gluons help us better understand quark confinement. Consider pulling a meson apart by slowly separating the quark from the antiquark. There is an attractive strong force between the quark and the antiquark, carried by a field of virtual gluons. The self-interaction of the gluons pulls this field into a narrow tube or string of colour-field, which connects the quark with the anti-quark. The cross section of the string, and hence the energy per unit length of the string is approximately constant. When the quark and anti-quark are separated, the string is stretched and the potential energy increases linearly with separation. This phenomenon leads to a term in the strong potential $V(r)$ proportional to r, which then dominates at large separation (see §**??**, equation (**??**)).

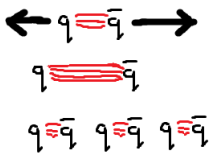

Meson production caused by rapidly separating quarks. A similar mechanism forms baryon-antibaryon pairs.

When sufficient energy has built up in the string it becomes energetically favourable for the string to break by dragging multiple quark-antiquark pairs out of the vacuum. The quarks and anti-quarks rapidly gather together into colour-neutral combinations – mesons or barons. It is those hadrons that are experimentally observed if a quark and an antiquark are forcibly separated. The relativistic 'headlight effect' squeezes the emitted hadrons into a narrow cone or 'jet' of hadrons.

Consider the high energy collision process

$$e^+ + e^- \rightarrow q + \bar{q}.$$

At high energy this process produces a rapidly separating quark-antiquark pair. Each quark leads to a jet of hadrons. The experimental verification of this can be seen in Figure 1. The jets indicate the directions, momenta and energies of the out-going quark and anti-quark.

Gluons are coloured particles so, like quarks, they cannot exist in isolation. Gluons cannot be seen directly, but their presence can be inferred. The gluon was discovered in reactions of the sort

$$e^+ + e^- \rightarrow q + \bar{q} + g$$

where the outgoing high-momentum gluon is emitted at large angle from both the quark and the anti-quark. Since each of the three outgoing particles is coloured, each must pull quarks and anti-quarks out of the vacuum to form neutral hadrons. The result is an event containing three jets of hadrons, each following the direction of one of the three out-going coloured particles (Figure 2).

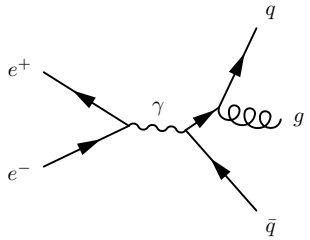

Feynman diagram with gluon emission leading to a three-jet event.

3.1 Deep inelastic scattering

Though it seems to be impossible to isolate an individual quark, it is still possible to perform scattering experiments at the quark level. Consider a high-momentum electron scattering from a proton. A high-momentum electron can resolve distances of order $\frac{\hbar}{p}$. If the momentum is larger than about $1\,\text{GeV}$ (so that its de Broglie wavelength λ is much smaller than the radius of the proton) then it will not scatter

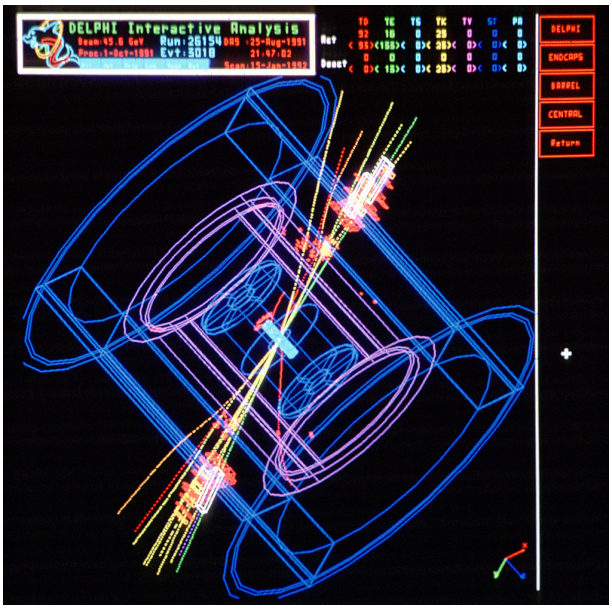

Figure 1: A two-jet event in the Delphi detector at a electron-positron centre-of-mass energy close to 100 GeV. © CERN 1992.

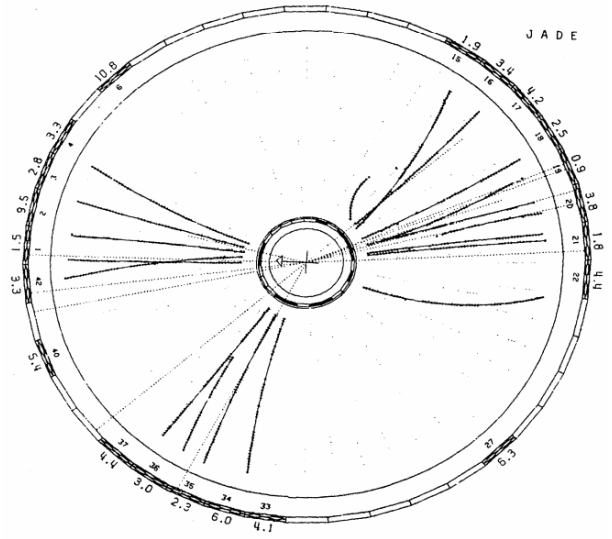

Figure 2: A three-jet event in the JADE detector. The process $e^+ + e^- \rightarrow q + \bar{q} + g$ leads to three jets, one from each of the three coloured particles.

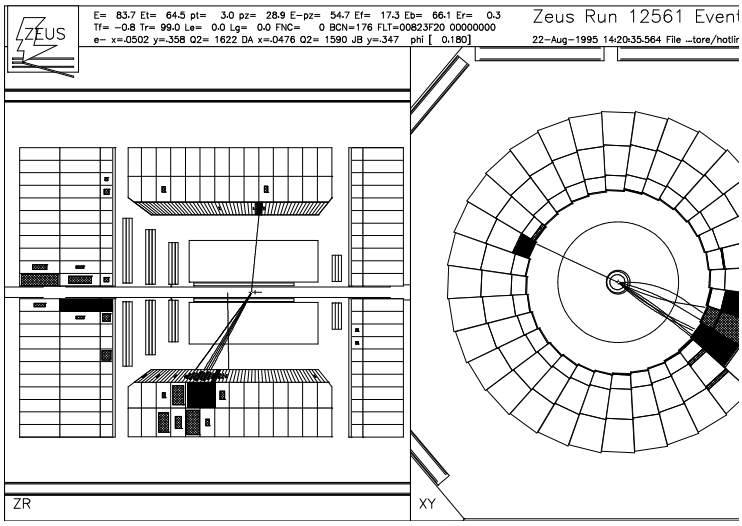

Figure 3: Longitudinal (left) and transverse (right) event display showing the debris from a deep inelastic scattering event, as measured in the Zeus detector. The electron has entered the detector from the left hand side on the transverse view, and the proton from the right hand side. The scattered electron forms an isolated track, terminating in an energy deposit in the calorimeter. A jet of hadrons recoils against the scattered electron.

coherently from the proton as a whole. Instead it will resolve the proton's internal structure — and at sufficiently high momentum will act as if it has been scattered from one of the constituent quarks.

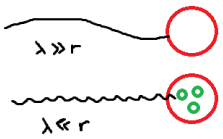

A high momentum probe can resolve the substructure of the proton.

The scattering of a probe from a quark inside a hadron is known as deep inelastic scattering.[1]

At high energies, the energy of the out-going quark will be much larger than typical hadron masses. As the quark is pulled away from the other quarks, some the energy is transferred into the string of gluon field lines that connect the quark and the anti-quark. Eventually the energy is high enough to pull quark-antiquark pairs out of the vacuum. What we observe is a jet of hadrons pointing in the direction of the original outgoing quark. The unscattered 'spectator' quarks in the proton also form a coloured state, and so must also form into hadrons.

Scattering experiments of this sort were performed at the HERA electron-proton collider, near Hamburg. Protons were accelerated to energy of $E_p = 920\,\text{GeV}$, and electrons to energies of $E_e = 27.5\,\text{GeV}$. A quark is scattered out of the proton by the incident electron. In Figure 3 we can see a display of such a scattering event. The scattered electron produces a single track terminating in an energy deposit in the calorimeter. Recoiling against that electron is a jet of hadrons pointing in the direction of the scattered quark. A further jet of hadrons can be seen in the transverse section close to the beam line, formed from the proton di-quark remnant.

[1] Deep because we are probing deep inside the hadron.

Though the individual quark cannot be observed, the jet of hadrons tell us about its direction and momentum, and the electron behaves as if it were scattering from a point-like spin-half particle.

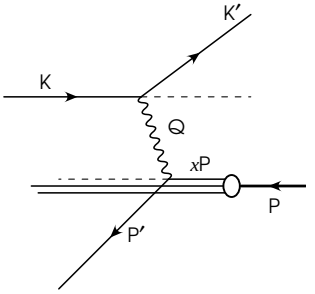

Scattering of an electron (momentum K→K′) from quark (momentum xP) within a proton (momentum P).

The force is transmitted by a virtual photon of momentum Q = K − K′. Note that unusually here the incoming proton is on the right side and the outgoing fragments of that proton are on the left side of the diagram.

3.2 Further evidence for quarks and colour: R

Further evidence for the existence of both quarks and colour can be found in when quark-antiquark pairs are created in electron-positron scattering. Consider the ratio

$$R \equiv \frac{\sigma(e^+ + e^- \to \text{hadrons})}{\sigma(e^+ + e^- \to \mu^+\mu^-)}.$$

Each process involves the collision of an electron and its anti-particle, a transition through a short-lived virtual photon.

The denominator comes from

$$e^+ + e^- \to \gamma^* \to \mu^+\mu^-$$

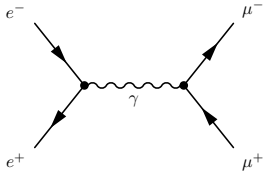

Feynman diagram for electron-positron annihilation, via a virtual photon to a muon-antimuon pair.

At the quark level the numerator comes from

$$e^+ + e^- \to \gamma^* \to q + \bar{q}$$

where various different quark flavours may contribute, depending on the centre-of-mass energy available.

The coupling of the photon to the quark i is proportional to the quark charge $\mathcal{Q}_i$. The Feynman diagram for the amplitude for production of the quark-antiquark pair is therefore proportional to $\mathcal{Q}_i$. The rate will therefore be proportional to the mod-squared of the amplitude, and so

$$\sigma_i \propto \Gamma_i \propto \mathcal{Q}_i^2$$

The corresponding amplitude for the creation of the muon-antimuon pair will look the same, but with $\mathcal{Q}(\mu) = 1$

The density-of-states factor for the muon and the quarks are also very similar, provided that $E \gg m$, so that $E \approx p$ for each out-going particle. The main difference in the density of states is that there are three different colours of quarks for any spin and momentum state, so the total density of states for any quark flavour is a factor of three larger than for the corresponding muon. We therefore expect that the value of the ratio will be

$$R = \frac{3 \times \sum_i \mathcal{Q}_i^2}{1 \times 1^2}$$

where the sum is over the $q\bar{q}$ states available at the given centre-of-mass energy, that is those with $m_q < E_{\text{cm}}/2$. Measurements confirm that as the threshold energy for production of new $c\bar{c}$ and $b\bar{b}$ states is passed, the value of R increases as expected. The value of R is also consistent with the three different colours of quarks.

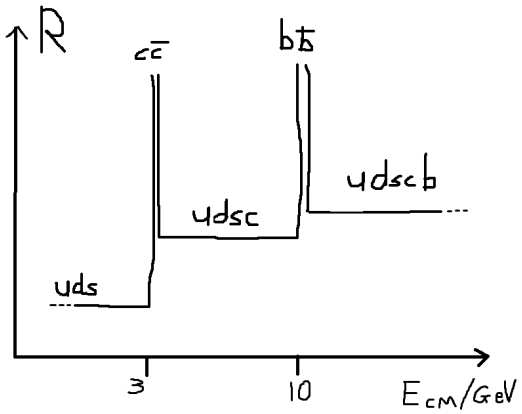

Figure 4: Sketch of the ratio of cross sections $R \equiv \frac{\sigma(e^+ + e^- \to \text{hadrons})}{\sigma(e^+ + e^- \to \mu^+ \mu^-)}$.

4 The weak interaction: W and Z particles

The weak interaction is mediated by three particles, the charged $W^\pm$ bosons and the neutral Z^0 boson. The W^+ and W^- are antiparticles of one another, while the Z^0, like the photon, is its own antiparticle.

The W and Z particles are spin-1 bosons. The weak force is very short range as a result of their large masses.

$$\boxed{m_W = 80.3\,\text{GeV}} \qquad \boxed{m_Z = 91.2\,\text{GeV}}$$

which from their approximate range $\hbar c/mc^2$ is about 2×10^{-3} fm, which is about 1000 times smaller than the size of the proton.

The weak force is responsible for all flavour-changing reactions. The only particles capable of changing quark flavour are the $W^\pm$ bosons. For example the beta decay of the neutron

$$n \to p + e^- + \bar{\nu}_e$$

requires us to change a d quark into a u quark. This can occur with the emission of a highly virtual W^- which subsequently produces an electron and a neutrino. For this reaction to proceed it is clear that the W boson must be able to interact both with the quarks and with the leptons.

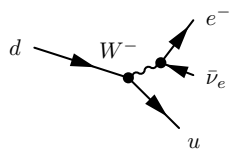

β decay

The emission or absorption of a $W^\pm$ particle changes an up-type quark (u, c or t) into a down-type quark (d, s, or b) or vice versa. For example, the decay of a K^+ meson

$$K^+ \to \pi^0 + \pi^+$$

at the quark level is mediated by a virtual W boson

$$u + \bar{s} \to u + \bar{u} + \left(W^+ \to u + \bar{d}\right).$$

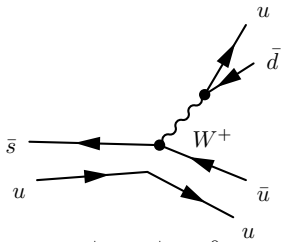

$K^+ \to \pi^+ + \pi^0$

The coupling of the W boson to leptons is **universal**. The vertex factor for each is takes the same value of g_W. This means that the W^- is equally likely to decay to any of the three lepton species:

$$\begin{aligned} W^- &\rightarrow e^- + \bar{\nu}_e \\ W^- &\rightarrow \mu^- + \bar{\nu}_\mu \\ W^- &\rightarrow \tau^- + \bar{\nu}_\tau. \end{aligned}$$

The coupling constants are equal, and the density of states factors are very similar since each of the decay products is highly relativistic, so the rates for each lepton flavour are identical.

A vertex involving a W and two quarks must include an upper $\mathcal{Q} = +\frac{2}{3}$ quark and a lower $\mathcal{Q} = -\frac{1}{3}$ quark. The vertices which include two quarks from the same generation dominate, while those involving transitions between generations are suppressed. The preference of the W boson for 'keeping it in the family' is one of the reasons why the concept of generations (or families) is useful.

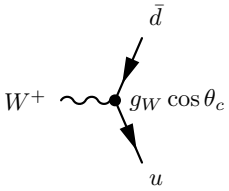

In the first and second generations the couplings for vertices within the same generation — i.e. the vertices for the (W, u, d) vertex or for the (W, c, s) vertex take the value

$$g_W \times \cos\theta_C,$$

where the θ_C, the **Cabibbo angle**, is about 13°.

The inter-generational couplings between the first and second generations – i.e. the vertex factors for the (W, u, s) vertex and the (W, c, d) vertex — are suppressed by the sine of the Cabibbo angle,

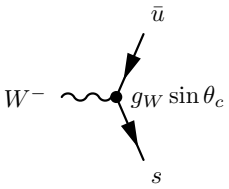

$$g_W \times \sin\theta_C.$$

The effect of this same-family favouritism can be seen, for example, when a hadron containing a charm quark decays, when it is likely to produce other hadrons containing strange quarks, since the (W, c, s) vertex is not Cabibbo suppressed.

An explanation for the relative sizes of the couplings can be found if we consider the down-type quarks to have weak interaction eigenstates, $|d'\rangle$ and $|s'\rangle$, each of which is a superposition of the two mass eigenstates $|d\rangle$ and $|s\rangle$. In the interaction basis the couplings of the W are diagonal, so the (W, u, d') and the (W, c, s') couplings each take the same value g_W, whereas the couplings for (W, u, s') and (W, c, d') are each zero.

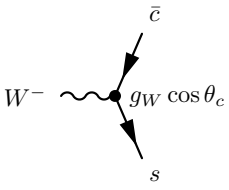

The flavour eigenstates $\{|d'\rangle, |s'\rangle\}$ in the primed basis must differ from the mass eigenstates $\{|d\rangle, |s\rangle\}$ in the un-primed basis. This can be achieved by rotating the states by a matrix

$$\begin{pmatrix} |d'\rangle \\ |s'\rangle \end{pmatrix} = V_{\rm c} \begin{pmatrix} |d\rangle \\ |s\rangle \end{pmatrix}$$

where the 2×2 Cabibbo rotation matrix is given by

$$V_c = \begin{pmatrix} \cos\theta_c & -\sin\theta_c \\ \sin\theta_c & \cos\theta_c \end{pmatrix}.$$

Three-generation flavour mixing

In the diagram below the solid lines show the unsuppressed transitions, while the dashed and dotted lines show progressively more suppressed transitions for decays between quarks of all three generations.

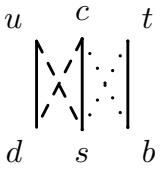

The three-generational extension of the Cabibbo matrix is the 3×3 unitary 'CKM' matrix,

$$V_{\rm CKM} \sim \left(\begin{array}{ccc} \square & \square & \cdot \\ \square & \square & \cdot \\ \cdot & \cdot & \square \end{array} \right).$$

where the larger boxes indicate larger couplings, and the dots show small couplings. The upper-left 2×2 block of the CKM matrix contains the mixing between the first two generations, which is also represented by the simpler 2×2 Cabibbo matrix.

The third generation is almost completely decoupled from the first two. Couplings involving either t or b any any of the quarks from the first two generations are very small. Top quarks almost always produce b quarks in when they decay. Hadrons containing b quarks have CKM suppressed decays and can travel macroscopic distances before they decay.

4.1 The Z^0 particle

The third weak boson is the Z^0. Like the $W^\pm$ bosons it is about 100 times heavier than the proton. Unlike the $W^\pm$ bosons it is electrically neutral.

The Z^0 also interacts with all of the fundamental fermions. Indeed since the neutrinos have no electrical or colour charge, interactions involving the weak force are the *only* way in which they may interact. The first evidence for the Z^0 boson was the discovery of scattering of neutrinos via the 'neutral current' exchange of a Z^0 boson.

The Z^0 does *not* change quark or lepton flavour, so there is for example no (u, c, Z^0) vertex. This is an example of the rule that there are 'no flavour-changing neutral currents' in the Standard Model. The branching ratios of the Z^0 to the different charged leptons are all consistent with one another, demonstrating that the couplings to each generation of leptons are equal.

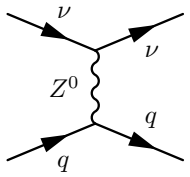

Neutral current neutrino scattering

4.2 Production and decay of the $W^\pm$ and Z^0 particles

The $W^\pm$ and Z^0 particles were first directly observed in 1983 in proton-antiproton collisions at the CERN Sp$\bar{\text{p}}$S proton-antiproton collider. The $p\bar{p}$ centre-of-mass energy of 540 GeV was sufficiently high that, even though the incoming (anti-)quarks carried only a fraction of the (anti-)proton momenta, collisions with $q - \bar{q}$ centre-of-mass energy close to the ~ 100 GeV mass of the W or Z were likely.

ℓ	$\mathcal{B}\left(Z^0 \to \ell^+ + \ell^-\right)$
e	$(3.363 \pm 0.004)\%$
μ	$(3.367 \pm 0.007)\%$
τ	$(3.370 \pm 0.008)\%$

The branching ratios of Z^0 boson to different charged leptons are all consistent with one another. [PDG(2008)].

In each case the intermediate vector bosons are created when a quark from the proton annihilates with an anti-quark from the anti-proton. To produce a Z^0 the quarks must be of the same flavour — either $u + \bar{u}$ or $d + \bar{d}$. To produce a W^+ or a W^-, the combinations $u + \bar{d}$ and $d + \bar{u}$ respectively are required.

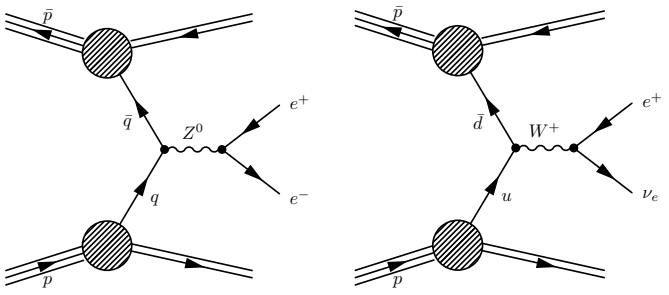

The diagrams above show the production of the Z^0 (left) and the W^+ boson (right) in proton-proton collisions, followed by their leptonic decays.

If the quark carries momentum fraction x_1 of the proton, and the anti-quark carries momentum fraction x_2 of the anti-proton, then to produce a Z^0 close to its mass

shell, where the cross section is largest, we require that

$$\begin{aligned} m_Z^2 &= (\mathsf{P}_q + \mathsf{P}_{\bar{q}})^2 \\ &= \mathsf{P}_q^2 + \mathsf{P}_{\bar{q}}^2 + 2\,\mathsf{P}_q \cdot \mathsf{P}_{\bar{q}} \\ &\approx 0 + 0 + 2x_1x_2\mathsf{P}_p \cdot \mathsf{P}_{\bar{p}} \\ &= x_1x_2 \times E_{CM}(p\bar{p}) \end{aligned}$$

Where $E_{CM}(p\bar{p})$ is the centre-of-mass energy of the proton antiproton system.

The W and Z particles were discovered in the leptonic decay modes. There are large backgrounds to the hadronic decay modes from elastic $q\bar{q}$ scattering through the strong interaction. Event displays of collisions producing Z and W bosons can be found in Figure 5.

The $W^{\pm}$ bosons then each decay to the fermions. For the W^+ these are

$$\begin{aligned} W^+ &\to u + \bar{d}' \\ W^+ &\to c + \bar{s}' \\ W^+ &\to e^+ + \nu_e \\ W^+ &\to \mu^+ + \nu_\mu \\ W^+ &\to \tau^+ + \nu_\tau \end{aligned}$$

The other possible quark-antiquark state, $t+\bar{b}$, is inaccessible for W bosons close to their mass shells, since the top quark is much heavier than the W boson. We have ignored the mixing in the quark sector, in which approximation the coupling of the W to each of the fermions is the same. The couplings to the fermions are universal in the flavour basis, but are mixed by CKM matrix factors in the mass–energy basis. Decays to the quark states are enhanced by a colour factor of 3, since the $q\bar{q}$ pair can be in any of the colour states $r\bar{r}$, $b\bar{b}$ or $g\bar{g}$.

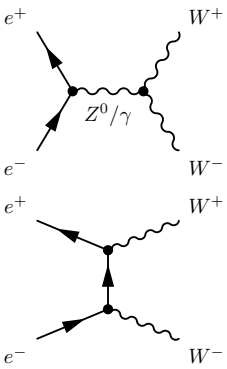

W production via a highly virtual γ or Z propagator (top) or via neutrino exchange (bottom).

Many of the most precise measurements of the W and Z bosons have been determined from in electron-positron collisions

$$e^- + e^+ \longrightarrow W^- + W^+$$

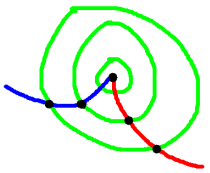

Tracks bending in the magnetic field.

Three different leading order Feynman diagrams contribute to this process (a) via a photon γ (b) via a Z^0 or (c) via ν_e exchange.

4.2.1 Particle detectors

General purpose particle detectors at colliders generally have a series of different layers surrounding the interaction point.

The inner part of the detector is used to track the trajectory of charged particles and measure their momenta as they bend in an externally applied magnetic field. The direction of curvature of the track indicates the sign of the charge, and the

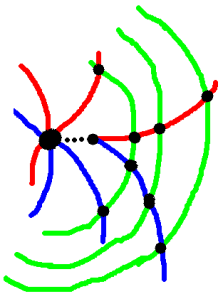

Secondary vertex reconstruction.

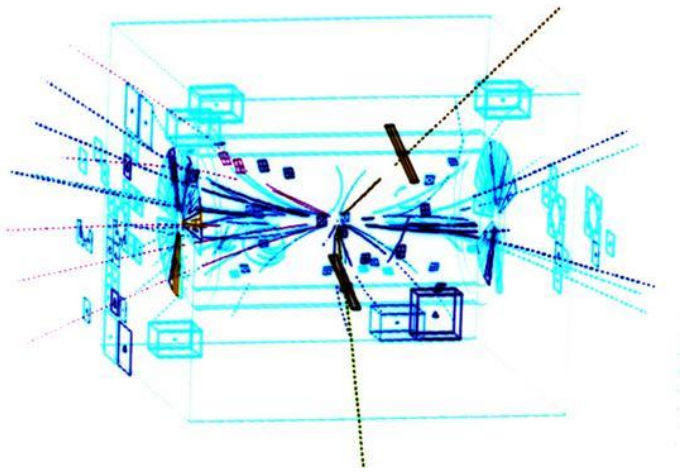

$q + \bar{q} \to Z^0 \to e^+ + e^-$

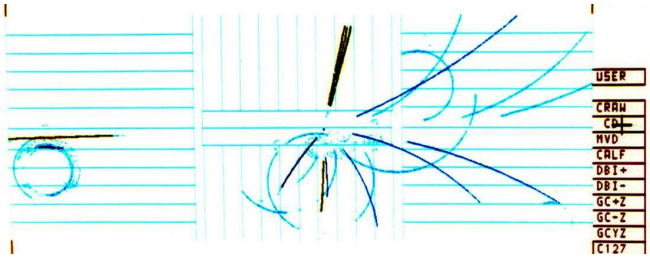

$q + \bar{q}' \to W \to \tau + \nu$

Figure 5: Event displays from the UA1 experiment for Z^0 production (top) and W production (bottom). In the top figure, the electrons follow in the direction of the black dotted lines. They leave straight, high-momentum tracks in the inner tracking detector and then are absorbed in the calorimeter, as indicated by the dark cuboids. In the bottom figure, the tau lepton from the W decay has itself decayed to three charged hadrons, visible as high-momentum straight tracks close to one another in the upper part of the plot. Other hadrons are also emitted from the proton remnants. These are more tightly curved tracks in the magnetic field.

radius of curvature R permits calculation of the component of the momentum $p_\perp$ perpendicular to the field

$$p_\perp = \mathcal{Q}BR.$$

Closest to the interaction point are usually high precision semiconductor pixel detectors, or microstrip detectors. By measuring tracks to precisions of order $10\,\mu$m, it's possible to reconstruct the position of the decay of particles with lifetimes as short ~ 100 ps. Charged particles traversing the semiconductor layers generate electron-hole pairs, allowing a current to flow.

Beyond the tracker are layers of **calorimeter** which are designed to stop the particles and convert their energies into electrical signal. Electromagnetic calorimeters rely on cascades caused by sequential Bremsstrahlung and pair creation in the electromagnetic field of an atomic nucleus:

$$e^\pm + \text{nucleus} \to e^\pm + \gamma + \text{nucleus}$$
$$\gamma + \text{nucleus} \to e^- + e^+ + \text{nucleus}$$

Electromagnetic calorimeters are effective at detecting (anti-)electrons and photons.

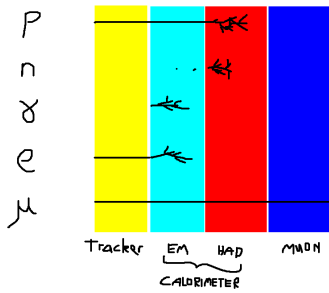

Different particles leave different signatures in the detector.

Hadronic calorimeters lie beyond the electromagnetic calorimeters, and are used to measure the energies of the long-lived baryons and mesons. The hadrons interact with the atomic nuclei via the strong interaction, producing inelastic scattering reactions such as

$$\begin{aligned} n + \text{nucleus} &\to n + \pi^0 + \text{nucleus} \\ p + \text{nucleus} &\to n + \pi^+ + \text{nucleus} \\ \pi^- + \text{nucleus} &\to \pi^- + \pi^+ + \pi^- + \text{nucleus} \\ \pi^+ + \text{nucleus} &\to \pi^+ + \pi^0 + \text{nucleus}. \end{aligned}$$

Rather like in the electromagnetic case, cascades of such interactions create large numbers of charged pions — the lightest strongly interacting particles — and photons from the subsequent decay $\pi^0 \to \gamma + \gamma$.

The final layer in the detector is usually a **muon tracker**. Muons are highly penetrating, and are the only particles to pass through the calorimeters. Most large muon detectors work by measuring the ionization caused in a gas by the passage of the muon. By bathing the muon detector in a magnetic field, the measurement of the muons' momenta can be improved.

4.2.2 The invisible width of the Z^0 boson

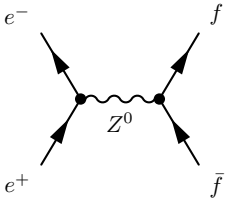

Production and decay of a Z^0 boson.

A beautiful experiment allows us to count the number of neutrino families to which the Z^0 decays, even though the neutrinos themselves are not directly observed.

Consider the production of Z^0 bosons via the resonant process

$$e^+ + e^- \to Z^0 \to f + \bar{f}$$

where f represents one of the Standard Model fermions, which could be a quark, a charged lepton or a neutrino. The total width of the Z^0 boson will be given by the sum of the partial widths,

$$\Gamma = \Gamma_{\rm Had} + \Gamma_{ee} + \Gamma_{\mu\mu} + \Gamma_{\tau\tau} + \Gamma_{\rm Invis}. \quad (1)$$

The decays to each of the five kinematically available quarks ($u\bar{u}$, $d\bar{d}$, $s\bar{s}$, $c\bar{c}$, $b\bar{b}$) all lead to hadronic final states. The partial width $\Gamma_{\rm Had}$ represents decays into any of these final states. The invisible width – the rate of decay to neutrinos – is given by the simple product of the partial width to a particular neutrino species $\Gamma_{\nu\nu}$ and the number of such species N_ν,

$$\Gamma_{\rm Invis} = N_\nu \times \Gamma_{\nu\nu},$$

since the Z^0 couples equally to each of the generations within the Standard Model.

The width of the Z^0 boson peak was precisely measured at the LEP $e^+ + e^-$ collider at CERN. The full width at half max of the Breit Wigner, Γ, was measured from the dependence of $\sigma_{\rm Had}$ on electron-positron centre-of-mass energy. The partial widths to each of the observable final states can each be calculated from their production cross sections at the Z^0 peak.

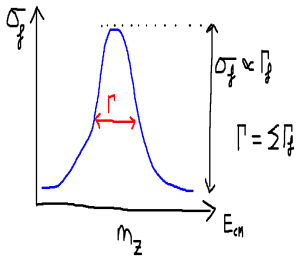

Cross section for $e^+ + e^- \to f + \bar{f}$ as a function of centre-of-mass energy.

Knowing of all of the other widths in (1), $\Gamma_{\rm Invisib}$ can be calculated. The partial width $\Gamma_{\nu\nu}$ is calculable from the related process of neutral-current scattering of neutrinos. Treating N_ν as an unknown, the following value was obtained:

$$N_\nu = 2.984 \pm 0.008,$$

consistent with the three generational model, and excluding the existence of another similar generation of particles.

4.3 Parity violation in the weak interaction

The strong and the electromagnetic interaction both respect parity. That is the part of the Hamiltonian that involves those interactions commutes with the parity operator, $\mathbb{P}$.

The parity operator generates the transformation of inversion of coordinates

$$\mathbb{P} : \mathbf{x} \mapsto -\mathbf{x}.$$

Under the parity operation, polar vectors such as those for position $\mathbf{x}$, velocity $\mathbf{v}$, momentum $\mathbf{p}$, and electric field $\mathbf{E}$ pick up a minus sign. Axial vectors such as angular momentum $\mathbf{J}$, and magnetic field $\mathbf{B}$ remain unchanged. An example of an axial vector is the orbital angular momentum L which transforms as follows:

$$\mathbf{L} \overset{\mathbb{P}}{\mapsto} L' = \mathbf{x}' \times \mathbf{p}' = -\mathbf{x} \times -\mathbf{p} = \mathbf{x} \times \mathbf{p} = \mathbf{L},$$

that is, like J and B, it is unmodified.

The electromagnetic laws of Maxwell and Lorentz remain valid after the parity operation. For example under a parity transformation, the Lorentz force law $\mathbf{F} = q(\mathbf{E} + \mathbf{v} \times \mathbf{B})$ transforms to

$$\begin{aligned} \mathbb{P}(\mathbf{F}) &= \mathbb{P}(q(\mathbf{E} + \mathbf{v} \times \mathbf{B})) \\ -\mathbf{F} &= q(-\mathbf{E} + -\mathbf{v} \times +\mathbf{B}) \\ \mathbf{F} &= q(\mathbf{E} + \mathbf{v} \times +\mathbf{B}) \end{aligned}$$

which remains a valid statement of the same law.

This may seem obvious, but becomes much less so when it is realized that unlike the electromagnetic and the strong forces, both of which are insensitive to the parity operation, the weak interaction is peculiar in that the law that describes it does not remain valid after a parity operation.

4.3.1 The discovery of parity violation

A test for parity violation in the weak interaction was suggested in 1956 [Lee and Yang(1956)]. The proposed experiment involved the beta decay

$$^{60}\mathrm{Co} \rightarrow {}^{60}\mathrm{Ni} + e^- + \bar{\nu}_e.$$

The cobalt nucleus, which has $J^P = 5^+$, decays to the $J^P = 4^+$ nickel nucleus.

The cobalt is cooled to 0.01 K and immersed in a strong magnetic field $\mathbf{B}$ so that the nuclear spins are preferentially aligned along the magnetic field, due to a term in the Hamiltonian $-\boldsymbol{\mu} \cdot \mathbf{B}$. The directions of the outgoing beta electrons are then observed.

Consider the behaviour of the momentum vector $\mathbf{p}$ of the observed electrons and the magnetic moment direction $\boldsymbol{\mu}$ of the nuclei under the parity operation:

$$\begin{aligned} \mathbf{p} &\xrightarrow{\mathbb{P}} -\mathbf{p} \\ \boldsymbol{\mu} &\xrightarrow{\mathbb{P}} +\boldsymbol{\mu} \end{aligned}$$

After a parity operation the momentum vector is inverted, but the nuclear spin points in the same direction. Therefore if parity is to be conserved, there must be as many electrons emitted in the $+\mathbf{B}$ direction as in the $-\mathbf{B}$ direction.

What was observed [Wu et al.(1957)] was that the emission of beta particles was *not* symmetric with respect to the $\mathbf{B}$-field direction. When measured, there were more beta electrons found in the direction opposite to that of the nuclear spin. The implication is that parity is not conserved in this interaction. The weak force behaves differently after the parity operation.

Parity is not conserved in weak interactions

The laws of physics are therefore not the same after reflecting a system in a mirror.

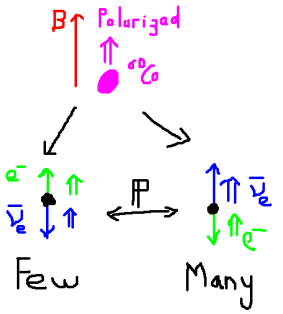

Angular momentum in the $^{60}\mathrm{Co}$ decay.

4.3.2 Parity and neutrino helicity

Another striking example of the violation of parity is found in the helicity of the neutrinos. Helicity h is the projection of the spin onto the direction of motion of a particle. Neutrinos are produced only with $h = -\frac{1}{2}$, and anti-neutrinos only with $h = +\frac{1}{2}$. No $h = +\frac{1}{2}$ neutrino has ever been observed. Since under the parity operation, helicity is reversed

$$h \xrightarrow{\mathbb{P}} -h,$$

we can infer that the laws which control the neutrino production cannot conserve parity, since if they did we should find as many $h = +\frac{1}{2}$ as $h = -\frac{1}{2}$ neutrinos.

$$h = \frac{\mathbf{S}\cdot\mathbf{p}}{|\mathbf{p}|}$$

	h	
ν	$-\frac{1}{2}$	$\xleftarrow{}$
$\bar{\nu}$	$+\frac{1}{2}$	$\xrightarrow{}$

The implication of parity violation is that nature has an inherent 'handedness', seen only in the weak decay. Left-handed particles feel the weak force more strongly than right-handed ones. The opposite is true for antiparticles: the weak force interacts with right-handed antiparticles rather than left-handed ones.

5 Neutrino Oscillations

There are three different types of neutrino, which we have labelled

$$\{\nu_e,\ \nu_\mu,\ \nu_\tau\}$$

according to the flavour of charged lepton they interact with via the W boson interaction.

But flavour is not necessarily 'good' quantum number — by which we mean a quantum number which is conserved. If lepton flavour is not strictly conserved then a neutrino that is born as an electron-type neutrino might not still be an electron-type neutrino later on. More precisely, if the flavour eigenstates are not eigenstates of the Hamiltonian, then flavour will not be conserved, and the amplitude to find the neutrino in a particular flavour eigenstate will be a time-dependent quantity.

Let us label the energy eigenstates according to their mass

$$\{\nu_1,\ \nu_2,\ \nu_3\}.$$

A neutrino is created as an electron-type neutrino if it is produced in association with an antielectron $W^+ \to \nu_e + e^+$. The amplitude $a(t)$ for it still to be an electron-type neutrino at some later time t is

$$a(t) = \langle \nu_e(t) | \nu_e(0) \rangle.$$

If flavour is conserved, then $|a(t)|^2 = 1$ for all t. However if the Hamiltonian does not conserve flavour then $|a|^2$ will be a time dependent quantity, and in general will oscillate with time.

Let us consider the simplified two-neutrino system. We label the flavour eigenstates $|\nu_e\rangle$ and $|\nu_\mu\rangle$ as mixtures of the the energy (i.e. mass) eigenstates $|\nu_1\rangle$ and $|\nu_2\rangle$

$$\begin{aligned} |\nu_e\rangle &= |\nu_1\rangle \cos\theta + |\nu_2\rangle \sin\theta \\ |\nu_\mu\rangle &= -|\nu_1\rangle \sin\theta + |\nu_2\rangle \cos\theta. \end{aligned}$$

where θ is the mixing angle.

Let the neutrino start off as an electron-type neutrino at its initial position $\mathbf{x} = 0$ when $t = 0$. At later times the neutrino's state $|\Psi\rangle$ is given by

$$|\Psi(L,T)\rangle = |\nu_1\rangle \cos\theta\, e^{-i\phi_1} + |\nu_2\rangle \sin\theta\, e^{-i\phi_2}$$

where

$$\phi_i = E_i T - |\mathbf{p}_i| L.$$

where, without loss of generality, we have reduced to single spatial dimension for the propagating wave. The amplitude for the initial (electron) neutrino to then be found as a muon neutrino can be found by bra-ing through with $\langle\nu_\mu|$,

$$\langle\nu_\mu|\Psi(x,t)\rangle = \sin\theta\cos\theta\left(e^{-i\phi_2} - e^{-i\phi_1}\right).$$

The flavour-change probability $P(\nu_e \to \nu_\mu)$ is then

$$|\langle\nu_\mu|\Psi(L,T)\rangle|^2 = \sin^2 2\theta\, \sin^2\left(\frac{\phi_1 - \phi_2}{2}\right)$$

If the masses of the two neutrinos are the same, then the phases ϕ_1 and ϕ_2 will remain in synch and no flavour change results. However if $m_1 \neq m_2$ then we have a phase change

$$\Delta\phi_{12} \equiv \phi_1 - \phi_2 = (E_1 - E_2)T - (|\mathbf{p}_1| - |\mathbf{p}_2|)\, L$$

To work out the phase difference in full we ought to use a wave-packet analysis, but we can quickly arrive at the correct answer by assuming[2] $|\mathbf{p}_1| = |\mathbf{p}_2|$, and expanding for $m \ll E$, to find

$$\begin{aligned} \Delta\phi_{12} &\approx |p|\left(\sqrt{1 + \frac{m_1^2}{|p|^2}} - \sqrt{1 + \frac{m_2^2}{|p|^2}}\right) L \\ &\approx \frac{m_1^2 - m_2^2}{2E} L. \end{aligned}$$

[2] If this makes you a little uncomfortable, it should. This is the 'textbook' method, but not terribly convincing, since it's hard to convince yourself that the state is in a momentum eigenstate. A little more confidence can be gained by noting that the expression for the phase difference could also have been written

$$\Delta\phi_{12} = (E_1 - E_2)\left(T - \frac{E_1 + E_2}{|\mathbf{p}_1| + |\mathbf{p}_2|} L\right) + \frac{m_1^2 - m_{,2}^2}{|\mathbf{p}_1| + |\mathbf{p}_2|} L.$$

Therefore had we chosen to demand that $E_1 = E_2$ or even $\beta_1 = \beta_2$ the first term would have vanished and we would have arrived at the same answer as under the equal-momentum assumption.

The probability $P(\nu_e \to \nu_\mu)$ is therefore (in SI units)

$$\boxed{P(e \to \mu) = \sin^2 2\theta \, \sin^2 \left(\frac{\Delta m^2 c^3 L}{4\hbar E} \right)} \tag{2}$$

where $\Delta m^2 = m_1^2 - m_2^2$. The survival probability $P(\nu_e \to \nu_e)$ is, for the two-state system, simply $1 - P(\nu_e \to \nu_\mu)$. In more convenient units the argument of the oscillation phase can be written

$$\frac{\Delta m^2 c^3 L}{4\hbar E} = 1.3 \frac{\Delta m^2}{\mathsf{eV}^2} \frac{L}{\mathsf{km}} \frac{\mathsf{GeV}}{E},$$

making it clear that for differences in mass-squared $\Delta m^2 \ll \mathsf{eV}^2$ the distance oscillations will happen over a length of many kilometers.

The masses of the neutrinos are very small, and so extremely difficult to measure directly. Cosmological constraints indicate that the sum of the three neutrino masses must be less than about 0.6 eV. We can find out about the (differences in squares of) masses of the three different neutrinos ν_1, ν_2 and ν_3 by examining the oscillations between the the three different flavours. Experiments over many kilometres are needed to search for such oscillations, otherwise the oscillation probability will be negligible. The long distances over which they are oscillating come from a combination of the near-degeneracy of the masses, and the neutrinos' large Lorentz gamma factors (of order 10^{12}), meaning that they are subject to a huge time dilation.

5.1 Solar neutrinos

The earliest indication of neutrino oscillations was found in **solar neutrinos**. The sun emits only electron-type neutrinos, through processes such as

$$p + p \to {}^2_1\mathrm{H} + e^+ + \nu_e$$

After they travel to earth we can capture the higher energy solar neutrinos as ν_e using isotopes like ${}^{37}\mathrm{Cl}$ in the inverse beta decay reaction

$$\nu_e + {}^{37}\mathrm{Cl} \to e^- + {}^{37}\mathrm{Ar}.$$

This reaction cannot occur for other neutrino flavour states, so any deficit in the expected amount of ${}^{37}\mathrm{Ar}$ will indicate that electron-type neutrinos have either disappeared or have oscillated into another flavour state.

The experiment was first performed in the Homestake Gold Mine in South Dakota using a 390,000 litre tank of dry-cleaning fluid, C_2Cl_4 [Davis et al.(1968)]. To perform the experiment, the team had to isolate about one atom of ${}^{37}\mathrm{Ar}$ produced per day in all that cleaning fluid, while working in a mine 1.5 km underground. The rate predicted by consideration of the solar nuclear reactions was 7.6 SNU, where one SNU (solar neutrino unit) is 10^{-36} captures per target atom per second. The observed rate was 2.56 SNU. Only about a third of the expected number of neutrinos was observed, indicating that the ν_e had oscillated into an equal mixture of ν_e, ν_μ and ν_τ by the time they reached earth.

Confirmation of the oscillation hypothesis was found from the Sudbury Neutrino Observatory in Ontario, Canada. SNO could detect three different reactions

$$\begin{aligned} \nu_e + D &\rightarrow p + p + e^- && (CC) \\ \nu_x + D &\rightarrow p + n + \nu_x && (NC) \\ \nu_x + e^- &\rightarrow \nu_x + e^- && (ES) \end{aligned}$$

where ν_x is any neutrino species, and D is a duterium nucleus ${}^2_1\mathrm{H}$. The charged current (CC) reaction is only sensitive electron-type neutrinos, while the neutral current (NC) and elastic scattering (ES) reactions each detect all three neutrino flavours. Comparison of the rates [SNO(2002)] shows that CC reactions are reduced to a third of what would be expected in the absence of neutrino oscillations. Both NC and ES reactions occur at the rate one would expect with or without reactions, showing that the total number of neutrinos is unchanged. The initially electron-type neutrinos are therefore oscillating into an approximately equal mixture of ν_e, ν_μ and ν_τ.

5.2 Atmospheric neutrinos

Neutrinos are also produced in the upper atmosphere when high-energy cosmic rays strike the upper atmosphere producing pions. The charged pions decay to muons, which decay to electrons, a sequence of reactions which emits neutrinos of both electron-type and muon-type flavours:

$$\begin{aligned} \pi^+ &\rightarrow \mu^+ + \nu_\mu \\ \mu^+ &\rightarrow e^+ + \bar{\nu}_\mu + \nu_e \end{aligned}$$

A corresponding reaction occurs for the negative pions.

Most of these neutrinos will pass through the earth unhindered. Occasionally we can see one if it happens to hit our target. A neutrino experiment sensitive to direction will see some neutrinos coming down from the atmosphere, which will have travelled only a few km. Those neutrinos which have passed through the earth, and travel up through the detector will have travelled up to about 13,000 km before we observe them. By recording the direction and flavour of the arriving neutrinos, an experiment can test the survival probability of the neutrino flavour (2) as a function of distance (or rather as a function of L/E).

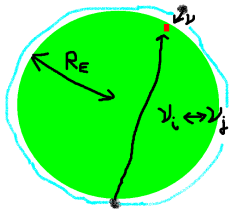

Upward-coming neutrinos have travelled further than have those coming directly down from the atmosphere.

The Super-Kamiokande experiment in Japan measured electron and muon type neutrinos of $\sim$ GeV energies using a 50 kton water Čerenkov detector. The experiment did not have sensitivity to tau-type neutrinos, since the neutrino energies were not high enough to produce τ leptons in charged current interactions. A deficit of muon neutrinos was found in the up-coming neutrinos which had travelled longer distances. The electron-type neutrinos were as would be expected in the absence of oscillations. These results indicate that flavour oscillations of the sort

$$\nu_\mu \rightleftharpoons \nu_\tau$$

were leading to loss of muon-type neutrinos. In the atmospheric experiment, the baseline L is too short for $\nu_e \rightleftharpoons \nu_\tau$ or $\nu_e \rightleftharpoons \nu_\mu$ oscillations.

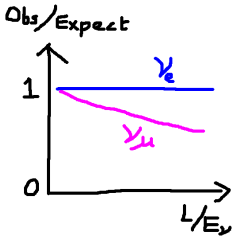

Super-Kamiokande found fewer upward coming muon neutrinos than expected.

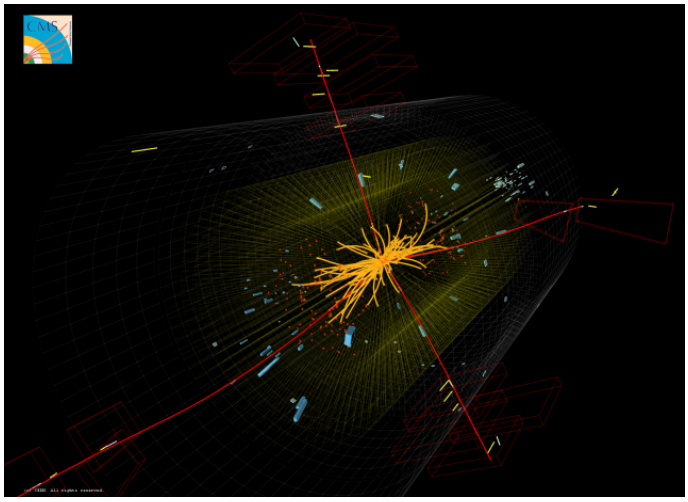

Figure 6: Display of a candidate Higgs boson event with the CMS detector. The red lines show muon tracks. The invariant mass of the four muons is equal to the mass of the Higgs boson.

6 The Higgs field

[non-examinable]

One particle, the spinless Higgs particle, plays a particularly special role in the Standard Model. It has unique properties in that it interacts with the other particles with couplings proportional to their masses.

To understand why the Higgs boson is necessary, consider the masses of the force-carrying particles. In quantum field theory, gauge bosons, the force-carrying particles, naturally arise as *massless* spin-1 excitations of the field carrying the force. This is fine for the photon and the gluons, which are indeed spin-1 bosons without mass. However the W and Z particles, though having spin 1 as expected, have large masses $\approx 100\,\text{GeV}$, so cannot so easily be explained as the massless excitations of the weak field. A mechanism is needed to provide the W and Z bosons with mass.

In the Higgs theory, the whole of space – the vacuum itself – is filled with a non-zero expectation value of the Higgs field. The particles which interact with this scalar field have modified properties. Those particles which interact with the field acquire masses according to their strength of interaction with the field. The W and Z particles, which would otherwise be massless, acquire their masses by interacting with the Higgs field in the vacuum. The photon is massless because it does not interact with the (electrically neutral) Higgs field.

The fundamental fermions – the quarks and leptons – also obtain their mass by interacting with this all-pervasive Higgs field. The top is the heaviest of the quarks exactly because it couples most strongly to the Higgs field. The electron is much lighter because its coupling to the Higgs field is much weaker.

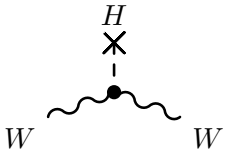

The Higgs field is non-zero in the vacuum (indicated by the cross). The vacuum interactions of the Higgs field with the W boson, of the sort shown in the diagram, give the W bosons its mass.

How does the vacuum get filled with Higgs field? Consider a 'Mexican hat' potential,

$$V(\varphi) = \mu^2 |\varphi|^2 + \lambda |\varphi|^4 ,$$

associated with a field φ, where $\mu^2 < 0$ and $\lambda > 0$. This potential has a local maximum at the origin (where $\varphi = 0$), and a minimum elsewhere where the fields are non-zero. The vacuum will settle into one of the states around the circle where V is minimum, meaning that φ takes a non-zero value in the vacuum. Thus the vacuum is filled with the field.[3]

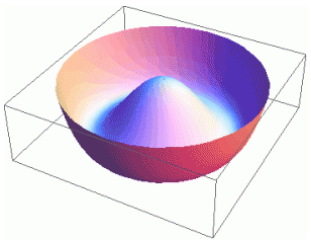

The potential associated with the Higgs field has a 'Mexican hat' shape. The vertical axis shows the potential $V(\varphi)$, as a function of the real and imaginary parts of the Higgs field φ. The potential has a local maximum at $\varphi = 0$, and a degenerate minimum at which $\varphi \neq 0$.

The excitation – or quantum – of the Higgs field is the Higgs boson. The Higgs boson is unique amongst the fundamental particles, in being a scalar – it has no intrinsic spin. It is responsible for a new Higgs interaction. This is a new type of force in nature, different from the electromagnetic, weak, strong and gravitational forces.

The couplings of the Higgs boson are fixed by the interactions of the Higgs field. The Standard Model particles must couple to the Higgs boson H with couplings proportional to their masses if they are to acquire their mass from the Higgs field. This means that the Higgs boson must couple strongly to heavy particles, light the top quark, and very weakly to light particles like the electron.

The discovery of the Higgs boson, was announced by the two large experiments at the Large Hadron Collider (LHC) in July 2012. Its mass was found to be close to 125 GeV and its properties consistent with being those expected from the Standard Model theory.[4]

6.1 Finding a Higgs boson

The Large Hadron Collider, where the Higgs boson was discovered, accelerates protons. Protons can be accelerated to the high energies required to make the Heavy Higgs boson. However protons are less than ideal for making Higgs particles, because the proton's constituent quarks – the up and down quarks – are the lightest of the quarks, and so couple only very weakly to Higgs boson. At the LHC the Higgs boson is dominantly made from gluon-gluon interactions. This seems counter-intuitive, since the gluon is massless, and so there is no direct coupling between the Higgs and the gluon at all. Instead the H must be made via an intermediate state - a triangular loop diagram,. The largest contribution comes from the top quark triangle diagram. The top quark can exist briefly in this virtual state, and has the advantage of a very large coupling to the Higgs boson.

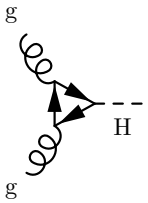

Production of a Higgs boson from a pair of gluons, via a top quark loop.

[3] In fact because a *particular* vacuum state is chosen by nature we break the gauge symmetry. This type of symmetry breaking happened in the very early universe, before the formation of hadrons. This is similar to what happens when directional symmetry is broken when a crystal freezes, selecting a particular direction.

[4] For a good series of articles explaining the discovery, try the special edition of 'Science' magazine published in December 2012: ATLAS paper and CMS paper.

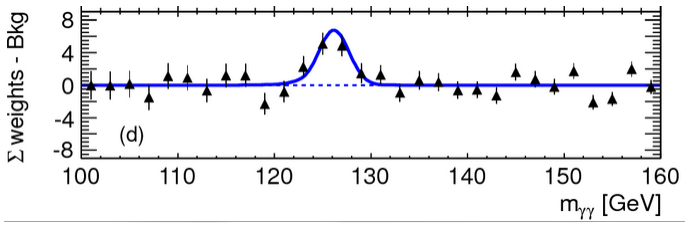

Figure 7: The discovery of the Higgs boson in the di-photon channel. The x-axis shows the di-photon invariant mass. The y-axis show the number of weighted events observed, after subtracting backgrounds. A peak can be observed at $m_{\mathrm{H}} \approx 125\,\mathrm{GeV}$. The width of the peak is dominated by experimental resolution.

The Higgs boson has been observed decaying in a variety of different ways, including

$$H \to W \ + \ W^* \to (e^+ + \nu_e) \ + \ (\mu^- + \bar{\nu}_\mu)$$
$$H \to Z \ + \ Z* \to (e^+ + e^-) \ + \ (\mu^+ + \mu^-)$$
$$H \to \gamma + \gamma$$
$$H \to \tau^- \ + \ \tau^+$$

The stars on the W and Z indicate that one or other of the W or Z particles is well off its mass shell. Both cannot be on-shell (or near-shell) since the Higgs boson mass $m_H \approx 125\,\mathrm{GeV}$ is less than either $2m_W$ or $2m_Z$. The Higgs boson has no spin, and is represented as dashed line (reserved for scalars) on a Feynman diagram. The photon γ is massless, the Higgs boson does not couple to it directly. Instead that decay must proceed via a loop diagram, typically involving a W boson or a t quark.

The ATLAS and CMS experiments each observe a clear (Figure 7) a characteristic Breit-Wigner peak in the histogram of the diphoton invariant mass $m_{\gamma\gamma}$ for events containing pairs of photons. This, together with similar evidence in decays to τ leptons, and W and Z bosons led to confirmation of the Higgs boson's existence.

Experiments are currently on-going to determine the couplings of the Higgs boson to all of the Standard Model fermions and bosons, and to measure the shape of the Higgs potential.

7 Beyond the Standard Model

[Non-examinable]

The Standard Model provides an extremely successful description of the fundamental constituents of nature as we observe them. However, it is known to have a limited range of validity, and it fails to address some of the most important questions about the matter and forces in our universe.

7.1 Gravity

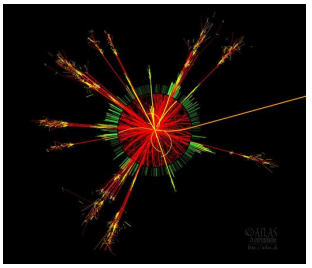

A simulation of a microscopic TeV-energy black hole evaporating through Hawking radiation at the LHC.

Gravity is notably absent from the Standard Model. While a description of gravity exists at the classical level in the form of General Relativity, this provides no microscopic explanation for gravity. We don't yet know what is transmitting the force at the quantum level. The difficulty in finding out is because gravity is so weak, despite it being the most familiar of the fundamental forces. Gravity can be incorporated within wider theories, such as string theories, however such theories do not yet make predictions that can be tested by experiment.

It has been suggested that a spin-2 *graviton* is responsible for the gravitational force. Such a particle might be detectable at extremely high energies, close to the Planck energy which in natural units is

$$E_{\text{Planck}} = \frac{1}{\sqrt{G_{\text{Newton}}}} \approx 10^{28}\,\text{eV}.$$

This energy scale is well beyond the reach of current colliders.

Some theories with extra dimensions of space suggest that gravity could become exponentially strong at TeV energies. In such theories gravitons (and/or microscopic black holes) could be observed at existing high-energy colliders, such as the LHC. Every time a collider reaches higher energies one of the first things one does is to perform a search for the effects of quantum gravity.

7.2 A theory of flavour

7.3 Matter / antimatter asymmetry

7.4 Unification of the forces?

7.5 The dark side of the universe

The Standard Model only accounts for the 5% of the matter-energy content of the universe. The astronomical and cosmologically evidence clearly favours a preponderance of Dark Matter (24% of the matter/energy content) and Dark Energy 71%.

The evidence for dark matter comes from a variety of sources, from the rotation curves of galaxies, to the formation of galaxies, to the acoustic oscillations in the early universe, to the evolution of the universe as a whole. So far we have no microscopic description for the source of the Dark Matter particles. We can infer some properties, for example we know that such particles cannot have electromagnetic interactions, otherwise they would not be 'dark'. They can't have strong interactions or they would already been observed as they bounce off our detectors. It's possible that they may interact only via the Weak or Higgs forces.

Figure 8: Dark matter detectors require low radioactive backgrounds, and are operated deep underground to shield them from cosmic rays. Some make use of copper from sunken Roman ships, which has particularly low induced radioactivity because it has been shielded from cosmic rays by the sea for centuries.

There are three major ways of looking for dark matter, all of which are competing to find it first. One method is to search for such particles being produced in colliders. The dark matter particles would not be observed directly, but would betray their presence through apparent non-conservation of energy or momentum, rather similar to the way neutrinos were first found.

An alternative search strategy is to look for the effects of naturally-occuring dark matter particles, as they bump into a very precise detector. The energy transmitted to the detector is observed as light, or as an electrical signal. Such detectors have to be radiologically pure, otherwise the energy signal from the dark matter particle would be lost in a background from nuclear interactions. They are also placed deep underground, in order to shield them from cosmic rays.

A third method is to search for Dark Matter particles annhilating against one another in space. Such annihilations could produce high energy Standard Model particles which we could be able to observe.

If dark matter does have Weak or Higgs interactions, it could be discovered soon via any of these methods.

7.5.1 Dark Energy

Dark Energy is believed to form the remaining 71% of the matter/energy contents of the universe. It takes the form of an energy density of empty space, and makes itself felt via the acceleration it causes in the expansion of the universe.

No good particle physics explaination yet exists for the Dark Energy. A non-zero energy of space is expected from quantum field theory, but unfortunately the calculated value is a factor of about 10^{120} too large. This has been called the worst prediction in physics. A value as large as that calculated would not allow structure to form in the universe. This has led some to speculate that there are many universes with different energy densities, and that we find ourselves, necessarily, in

one which is 'antropically selected' to favour the formation of structure, stars and intellegent life.

7.6 The hierarchy problem

7.7 Strings and things

Key concepts

- The fundamental matter particles are **spin-$\frac{1}{2}$ fermions**
- There are three families of **quarks**, and three corresponding families of **leptons**
- The forces and interactions between the quarks and leptons are mediated by **spin-1 bosons**
- The **electromagnetic force** is mediated by the neutral, massless photon γ
- The **strong force** is mediated by the eight massless gluons g which are themselves coloured, and so interact with one another.
- In deep inelastic scattering, a projectile scatters off the constituent quarks
- Free quarks are **not observed**, instead, when a quark is knocked hard, we find **jets** of colourless mesons and baryons.
- The **weak force** is mediated by the $W^{\pm}$ and Z^0 particles, which have large masses, and so only interact over $\sim 10^{-18}$ m
- The weak force violates conservation of parity
- The $W^{\pm}$ bosons are the only particles that can change quark flavour
- Neutrinos are observed to change flavour (oscillate) when travelling over long distances

Further reading

- B. Martin, *Nuclear and Particle Physics: An Introduction*
- W. S. C. Williams, *Nuclear and Particle Physics*
- K.S. Krane *Introductory Nuclear Physics*

.A Conservation laws

Operator	Strong	EM	Weak
Charge, $\mathcal{Q}$	✓	✓	✓
Baryon number	✓	✓	✓
Lepton number	✓	✓	✓
Parity, $\mathbb{P}$	✓	✓	×
Charge conjugation $\mathbb{C}$	✓	✓	×
$\mathbb{CP}$	✓	✓	almost
Strangeness	✓	✓	×
Charm	✓	✓	×
Bottomness	✓	✓	×
Isospin	✓	×	×

Table 3: Some important operators and their invariance properties for different interactions. A tick ✓ indicates that the interaction conserves that quantity. A cross × indicates that it does not conserve that quantity. The combined operation $\mathbb{CP}$ is almost conserved in the weak interaction.

References

[Hanneke(2008)] D. e. a. Hanneke, "New Measurement of the Electron Magnetic Moment and the Fine Structure Constant", *Phys.Rev.Lett.* **100** (2008) 120801, 0801.1134.

[Aoyama(2012)] T. e. a. Aoyama, "Tenth-Order QED Contribution to the Electron $g-2$ and an Improved Value of the Fine Structure Constant", *Phys.Rev.Lett.* **109** (2012) 111807, 1205.5368.

[PDG(2008)] **Particle Data Group** Collaboration, PDG, "Review of particle physics", *Phys. Lett.* **B667** (2008) 1.

[Lee and Yang(1956)] T. D. Lee and C. N. Yang, "Question of parity conservation in weak interactions", *Phys. Rev.* **104** Oct (1956) 254–258.

[Wu et al.(1957)] C. S. Wu *et al.*, "Experimental test of parity conservation in beta decay", *Phys. Rev.* **105** Feb (1957) 1413–1415.

[Davis et al.(1968)] J. Davis, Raymond *et al.*, "Search for neutrinos from the sun", *Phys.Rev.Lett.* **20** (1968) 1205–1209.

[SNO(2002)] **SNO Collaboration** Collaboration, SNO, "Direct evidence for neutrino flavor transformation from neutral current interactions in the Sudbury Neutrino Observatory", *Phys.Rev.Lett.* **89** (2002) 011301, nucl-ex/0204008.

